QUANTUM COMPUTATION WITH TRAPPED IONS

H. HÄFFNER[1,2], W. HÄNSEL[1], C. F. ROOS[1,2], P. O. SCHMIDT[1], M. RIEBE[1], M. CHWALLA[1], D. CHEK–AL–KAR[1] J. BENHELM[2], U. D. RAPOL[2], T. KÖRBER[1], C. BECHER[1,†], O. GÜHNE[2], W. DÜR[2,3], AND R. BLATT[1,2]

[1]*Institut für Experimentalphysik, Innsbruck, Austria*

[2]*Institut für Quantenoptik und Quanteninformation, Österreichische Akademie der Wissenschaften, Austria*

[3]*Institut für Theoretische Physik, Innsbruck, Austria*

[†] *Present address: Fachrichtung Technische Physik, D-66041 Saarbrücken, Germany*

Trapped ions can be prepared, manipulated and analyzed with high fidelities. In addition, scalable ion trap architectures have been proposed (Kielpinski *et al.*, Nature **417**, 709 (2001).). Therefore trapped ions represent a promising approach to large scale quantum computing. Here we concentrate on the recent advancements of generating entangled states with small ion trap quantum computers. In particular, the creation of W–states with up to eight qubits and their characterization via state tomography is discussed.

Keywords: entanglement; quantum information; ion traps

1. Introduction

Among the proposals for constructing a quantum computer, the approach based on trapped ions is currently one of the most advanced [1]. Here, the internal electronic states of trapped ions implement the qubits[2]. The state of the ions can be initialized, manipulated and read out with very high fidelities[2]. In addition, quantum information can be stored for up to 10 minutes as demonstrated by Bollinger and co–workers[3]. Thus, trapped ions are an ideal quantum memory. For processing this quantum information, however, a controllable quantum interaction between the qubits is also required.

In 1995, Cirac and Zoller realized that a string of ions trapped in a linear Paul trap provides a system where such an interaction may be realized[4]. Addressing individual ions with cleverly chosen laser pulses causes the conditional evolution of physically separated qubits. Thus, this is a system in which at one hand, the carriers of information are well separated from each other and the environment and on the other hand the interaction can be turned on and off at will. In addition, the size of resources necessary to control this system does not increase exponentially with the number of qubits[4]. This scalability is a necessary condition for a useful quantum computer.

Soon after the proposal by Cirac and Zoller in 1995, the ion storage group at NIST around David Wineland realized the key idea of the proposal —a controlled-NOT operation— [5] with a single Be^+–ion. Furthermore they demonstrated a few other two–qubit gates[6,7,8], entangled up to four ions in 2000[6], realized a so–called decoherence free subspace[9] and simulated a nonlinear beam–splitter[10].

In Rainer Blatt‘s group in Innsbruck the Deutsch–Josza algorithm was demonstrated in 2003 on a single Ca^+–ion[11], followed by the first implementation of a set of universal gates on a two–ion string[12].

Further milestones in ion–trap quantum computing were then experiments on quantum teleportation by both groups[13,14], an error correction protocol by the NIST–group[15] and entanglement of six ions[16]. Here we now concentrate on recent experiments[17] where up to eight ions were entangled in a so–called W–state[18,19].

Entanglement properties of two and three particles have been studied extensively and are very well understood. However, both creation and characterization of entanglement becomes exceedingly difficult for multi–particle systems.

To entangle numerous qubits, it is quite advantageous to use methods where the efficiency (e.g. the creation time) scales polynomially in the number of qubits. While this can be achieved, the full characterization of the entangled states still requires an exponentially increasing number of measurements. In spite of this, the availability of the density matrix such multi–particle entangled states together with the full information on these states in form of their density matrices is an important a test-bed for theoretical studies of multi–particle entanglement.

Here we obtain the maximum possible information on our entangled states by performing full characterization via state tomography[20]. With the density matrix at hand, we prove in a detailed analysis that they carry genuine four-, five-, six-, seven- and eight–particle entanglement, respectively.

2. Experiment

The generation of such W–states is performed in an ion–trap quantum processor[21]. We trap strings of up to eight $^{40}Ca^+$ ions in a linear Paul trap. Superpositions of the $S_{1/2}$ ground state and the metastable $D_{5/2}$ state of the Ca^+ ions (lifetime of the $|D\rangle$–level: $\tau \approx 1.16$ s) represent the qubits. Each ion–qubit in the linear string is individually addressed by a series of tightly focused laser pulses on the $|S\rangle \equiv S_{1/2}(m_j = -1/2) \longleftrightarrow |D\rangle \equiv D_{5/2}(m_j = -1/2)$ quadrupole transition employing narrow-band laser radiation near 729 nm. Doppler cooling and subsequent sideband cooling prepare the ion string in the ground state of the center–of–mass vibrational mode. Optical pumping initializes the ions' electronic qubit states in the $|S\rangle$ state. After preparing an entangled state with a series of laser pulses, the quantum state is read out with a CCD camera.

The entangled states prepared in the experiments are W–states[18,19]. An N–particle W–state

$$|W_N\rangle = (|D\cdots DDS\rangle + |D\cdots DSD\rangle$$
$$+|D\cdots DSDD\rangle + \cdots + |SD\cdots D\rangle)/\sqrt{N} \tag{1}$$

consists of a superposition of N states where exactly one particle is in the $|S\rangle$–state while all other particles are in $|D\rangle$.

The W–states are efficiently generated by sharing one motional quantum between the ions with partial swap–operations[17]. The time needed for entangling procedure is about 1 ms, while the cooling and read–out take 14 ms and 4 ms, respectively.

2.1. *State tomography*

Full information on the N–ion entangled state is obtained via quantum state reconstruction. For this we expand the density matrix in a basis of observables[23] and measure the corresponding expectation values. We employ additional laser pulses to rotate the measurement basis prior to state detection to accomplish the required basis rotation[20]. We use 3^N different bases and repeat the experiment 100 times for each basis. For $N = 8$, this amounts to 656 100 experiments and a total measurement time of 10 hours. To obtain a positive semi–definite density matrix ρ, we follow the iterative procedure outlined by Hradil *et al.*[24] for performing a maximum–likelihood estimation of ρ. The reconstructed density matrix for $N = 8$ is displayed in Fig. 1. To retrieve the fidelity $F = \langle W_N|\rho|W_N\rangle$, we adjust the local phases such that F is maximized. The local character of those transformations implies that the amount of the entanglement present in the system is not changed. We obtain fidelities $F_4 = 0.85, F_5 = 0.76$, $F_6 = 0.79$, $F_7 = 0.76$ and $F_8 = 0.72$ for the 4,5,6,7 and 8–ion W–states, respectively.

One important issue is to estimate the uncertainty the density matrix elements and of quantities derived from it. This is achieved with a Monte Carlo simulation: Starting from the reconstructed density matrix, we simulate up to 100 test data sets taking into account the major experimental uncertainty, i.e. quantum projection noise. Then the test sets are analyzed and we can extract probability distributions for all observables from the resulting density matrices.

Table 1 lists the expectation values for witness operators. An entanglement witness[25,26] is an operator which has for all separable states a positive expectation value. Thus a negative expectation value proves that genuine multi–partite entanglement is present. We have constructed such entanglement witnesses for our produced states and thus verified that they are genuinely N–partite entangled. Details can be found in Ref. [17].

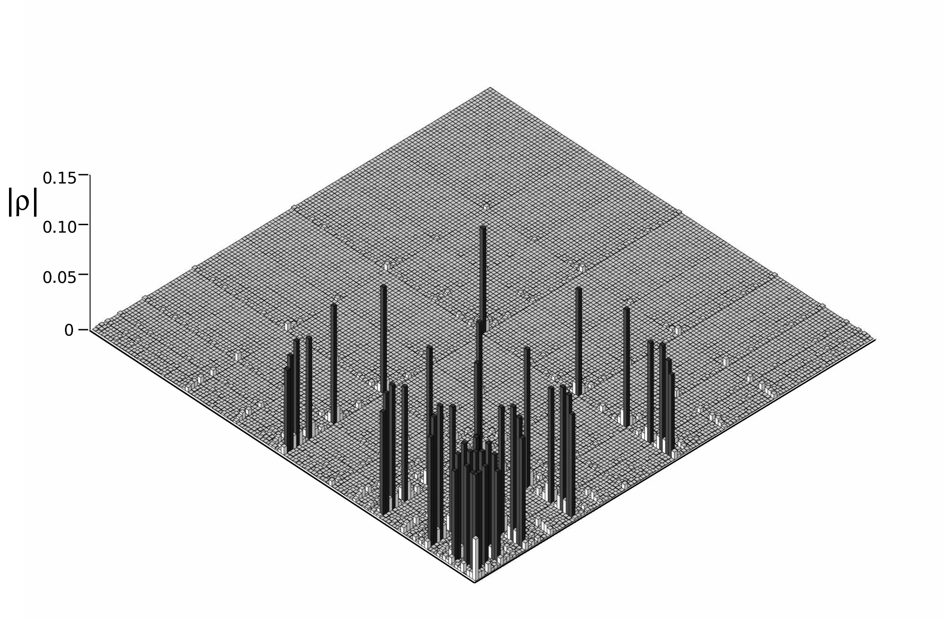

Figure 1. Absolute values of the reconstructed density matrix of a $|W_7\rangle$–state as obtained from quantum state tomography. Ideally, the dark entries have all the same height of $\frac{1}{7}$, the bright bars indicate imperfections. The state at the bottom corner corresponds to $|DDDDDDD\rangle$

.

Table 1. Entanglement properties of ρ_N. First row: Fidelity after properly adjusting local phases. Second row: Expectation value of the witnesses $\tilde{\mathcal{W}}_N$ (for $N = 8$ we used additionally local filters). For completeness we also analyzed the data published previously in Ref. 22 for $N = 3$.

	$N = 3$	$N = 4$	$N = 5$	$N = 6$	$N = 7$	$N = 8$
F	0.824	0.846 (11)	0.759 (7)	0.788(5)	0.763 (3)	0.722 (1)
$\mathrm{tr}(\tilde{\mathcal{W}}_N \rho_N)$	−0.532	−0.460 (31)	−0.202 (27)	−0.271 (31)	−0.071 (32)	−0.029 (8)

3. Experimental Imperfections

For an investigation of the experimental imperfections and scalability, we simulate the preparation procedure by solving the Schrödinger equation with the relevant imperfections.

We identify four major sources of deviations from the ideal W–states: addressing errors, imperfect optical pumping, non–resonant excitations, and laser frequency noise. The trap frequency influences these experimental imperfections diametrically: for example, to keep the addressing error reasonably low [i.e. less than 5%, where the addressing error is defined as the ratio of the Rabi–frequencies between the addressed ion and the neighboring ion(s)], we adjust the trap frequency such that the inter–ion distance in the center of the ion string is about 5 μm. However, for large N the required trap relaxation implies that the sideband transition frequency moves closer to the carrier transition frequency. Thus the strong laser pulses driving the weak sideband transition cause more off–resonant excitations on the carrier transition, which in turn spoil the obtainable fidelity. Therefore we reduce the laser power for driving the sideband, which then results in longer preparation times and leads to an enhanced susceptibility to laser frequency noise. For $N = 8$ we used 0.813 MHz for the center-of-mass frequency and 380 μs for a 2π–pulse on the blue sideband.

For the simulations we approximate the ions only as two-level systems and include only the first three levels of the center-of-mass excitation. For a serious analysis of the imperfections this is by no means sufficient as e.g. no environment is included. Still, the simulation time for the generation of a $|W_8\rangle$–state under these idealized conditions is already 20 minutes on a 3 GHZ processor using matlab. As the computational time for the simulations scales with 4^N, it is quite demanding to include a reasonable environment or even use a density matrix approach. The fidelity reduction of $|W_6\rangle$ for the different imperfections are as follows: 0.1 (addressing error), 0.07 (off–resonant excitations), 0.04 [laser frequency noise (200 Hz rms)]. Another possible error source is imperfect ground state cooling. Intensity noise of the 729–laser ($\Delta I_{\max}/I \approx 0.03$) does not contribute significantly. Finally, we experimentally observed non–ideal optical pumping which can result in a reduction of 0.02 of the fidelity per ion. For $N \geq 6$, we therefore minimize the errors due to optical pumping and a part of the addressing errors by checking the initialization procedure with a detection sequence . In addition, we switched the blue-sideband pulses adiabatically with respect to the trap frequency to minimize off–resonant excitations.

Thus for the $|W_6\rangle$–state used for the analysis in Tab. 1 the expected fidelity should be on the order of 0.91 as only addressing errors (significantly reduced by the conditional check after the initialization procedure (0.05)) and laser frequency noise (0.04) contribute to the imperfect fidelity. Even though it is hard to estimate the fidelity for $N = 8$ it seems that the discrepancy between the estimations and the experiment is even larger for $N = 8$.

If one looks closely at our produced density matrices (they are made available as supplementary material in Ref. [17], see also Fig. 1) the relatively strong occupation of the $|DD \cdots D\rangle$ stands out. This is not expected at all from the simulations. Future investigations will reveal whether this discrepancy is due mistakes in the pulse sequence, some unexpected short comings or whether some interesting physics is missing in the simulations.

4. Conclusion

In this contribution, we have presented experiments on W–states with up to eight ions. Methods to characterize the states and experimental imperfections are discussed. Even though the experimental system under investigation seems well understood, the quantitative behavior is not reproduced properly by the simulations.

Acknowledgments

We gratefully acknowledge support by the Austrian Science Fund (FWF), by the European Commission (SCALA, QGATES, CONQUEST PROSECCO, QUPRODIS and OLAQUI networks), by the Institut für Quanteninformation GmbH, the DFG, and the ÖAW through project APART (W.D.). This material is based upon work supported in part by the U. S. Army Research Office. We thank P. Pham for the pulse modulation programmer and A. Ostermann, M. Thalhammer and M. Ježek for the help with the iterative reconstruction.

References

1. Army Research Office ARDA quantum computation roadmap: http://qist.lanl.gov/qcomp_map.shtml
2. D. Wineland, C. Monroe, W. Itano, D. Leibfried, B. King, D. Meekhof, Journal of Research of the National Institute of Standards and Technology **103**, 259 (1998).
3. J. Bollinger, D. Heinzen, W. Itano, S. Gilbert, D. Wineland, IEEE Trans. Instrum. Meas. **40**, 126 (1991).
4. I. Cirac, P. Zoller, Phys. Rev. Lett. **74**, 4091 (1995).
5. C. Monroe, D. Meekhof, B. King, W. Itano, D. Wineland Phys. Rev. Lett. **75**, 4714 (1995).
6. C.A. Sackett *et al.*, Nature **404**, 256 (2000).
7. B. DeMarco *et al.*, Phys. Rev. Lett. **89**, 267901 (2002).
8. D. Leibfried *et al.*, Nature **422**, 412 (2003).
9. D. Kielpinski, V. Meyer, M.A. Rowe, C.A. Sackett, W.M. Itano, C. Monroe, D. Wineland, Science **291**, 1013 (2001).
10. D. Leibfried *et al.*, Phys. Rev. Lett. **89**, 247901 (2002).
11. S. Gulde *et al.* Nature **421**, 48 (2003).
12. F. Schmidt-Kaler *et al.*, Nature **422**, 408 (2003).
13. M.D. Barrett *et al.*, Nature, **429**, 737 (2004).
14. M. Riebe *et al.*, Nature, **429**, 734 (2004).
15. J. Chiaverini *et al.* Nature **432**, 602 (2004).
16. D. Leibfried *et al.* Nature **438**, 639 (2005).
17. H. Häffner *et al.* Nature **438**, 643 (2005).
18. A. Zeilinger, M.A. Horne, D.M. Greenberger, Higher-order quantum entanglement. NASA Conf. Publ. **3135**, pp 73–81 (1992).
19. W. Dür, G. Vidal, J.I. Cirac, Phys. Rev. A **62**, 062314 (2000).
20. C.F. Roos *et al.*, Phys. Rev. Lett. **92**, 220402 (2004).
21. F. Schmidt–Kaler *et al.*, Appl. Phys. B **77**, 789–796 (2003).
22. C.F. Roos *et al.*, Science **304**, 1478–1480 (2004).
23. U. Fano, Rev. Mod. Phys. **29**, 74–93 (1957).
24. Z. Hradil, J. Reháček, J. Fiurášek, M. Ježek, Lect. Notes Phys. **649**, 59–112 (2004).
25. M. Horodecki, P. Horodecki, R. Horodecki, Phys. Lett. A **223**, 1–8 (1996).
26. M. Bourennane *et al.*, Phys. Rev. Lett. **92**, 087902 (2004).